

1	تصميم صفائح تثبيت طرفي العظم مع تقليل تأثير الحماية من الإجهاد باستخدام تحسين
2	الطوبولوجيا
3	اسم وكنية الباحث الاول مسبوقة صفته العلمية المختصرة (م.، د.، أ.د...)) ^١ ، اسم وكنية الباحث
4	الثاني ٢، اسم وكنية الباحث الثالث ٣
5	¹ الصفة العلمية، المركز البحثي أو الجامعة، التخصص الدقيق، البريد الإلكتروني (للباحثين في
6	جامعة دمشق البريد الإلكتروني الخاص بالجامعة للباحث)
7	² الصفة العلمية، المركز البحثي أو الجامعة، التخصص الدقيق، البريد الإلكتروني (للباحثين في
8	جامعة دمشق البريد الإلكتروني الخاص بالجامعة للباحث)
9	^٣ الصفة العلمية، المركز البحثي أو الجامعة، التخصص الدقيق، البريد الإلكتروني (للباحثين في
10	جامعة دمشق البريد الإلكتروني الخاص بالجامعة للباحث)
11	* توضع علامة النجمة فوق اسم الباحث الذي تتم المراسلات معه بغض النظر عن الترقيم او
12	ترتيب الاسماء (كباحث رئيسي - طالب دراسات عليا)
13	

الملخص:

يعرض المقال تحليل تأثير الحماية من الإجهاد (SSE) في صفائح تثبيت طرفي العظم، وأثاره الضارة على شفاء كسور العظام والحلول الممكنة لتقليلها. لقد تبين أنه يمكن تقليل SSE باستخدام ألواح مصنوعة من مواد ذات معامل مرونة منخفض (سبائك التيتانيوم، والبوليمرات القابلة للامتصاص الحيوي، وما إلى ذلك) أو عن طريق تحسين شكلها الهندسي. يتم تحليل الاحتمال الأخير بطريقة أكثر تفصيلاً مع التركيز بشكل خاص على تحسين الطوبولوجيا (TO) كأداة تحسين جديدة نسبياً تستخدم على نطاق واسع من قبل مجتمع الهندسة الطبية الحيوية. كمثال عملي، تم تطبيق TO باستخدام برنامج Comsol Multiphysics لحل مشكلة التصميم ثنائي الأبعاد صفائح تثبيت طرفي العظم. لقد تبين أن الصلابة الطولية للوحة المحسنة يمكن تقليلها بنسبة تصل إلى ٨٤٪ مقارنة بالتصميم الأولي غير الأمثل اعتماداً على قيمة التخفيض الموصوف للوزن المستخدم كقيد أثناء التحليل. يوضح التصميم الأمثل زيادة في الحد الأقصى لإجهاد فون ميزس، لكن التوزيع العام للضغوط يصبح أكثر اتساقاً مقارنة بالتصميم الأولي. يمكن تصنيع النموذج الأولي للصفحة المحسنة بسهولة باستخدام القطع بالليزر أو آلة التفريغ الكهربائي للأسلاك.

14 تاريخ الايداع
15 تاريخ القبول



16
17
18 حقوق النشر: جامعة دمشق
19 سورية، يحتفظ المؤلفون
20 بحقوق النشر بموجب CC BY-
21 NC-SA

22
23
24
25
26
27

Design Of Osteosynthesis Plates With Reduced Stress Shielding Effect Using Topology Optimization 29 30

DSc Dmitry Stepanenko¹, Hanna Bileichyk², Viktoryia Akhremchyk³, MSc Iskandar Mudinov⁴, PhD Heorhi Viarshyna⁵, Denis Bodyak⁶ 31
32

¹ Professor, Department “Design and Production of Instruments”, Belarusian National Technical University, dstepanenko@bntu.by 33
34

² Student, Department “Design and Production of Instruments”, Belarusian National Technical University, hanna0401@gmail.com 35
36

³ Student, Department “Design and Production of Instruments”, Belarusian National Technical University, victoriaakhremchik@gmail.com 37
38

⁴ PhD Student, Department “Design and Production of Instruments”, Belarusian National Technical University, mudinov.iskandar@mail.ru 39
40

⁵ Director, State Enterprise “Science and Technology Park of BNTU “Polytechnic”, gavershina@bntu.by 41
42

⁶ Engineer, State Enterprise “Science and Technology Park of BNTU “Polytechnic”, denis.bodyak@park.bntu.by 43
44

Abstract: 45

The article presents analysis of stress shielding effect (SSE) in osteosynthesis plates, its adverse effects on healing of bone fractures and possible solutions for its minimization. 46
47
It is shown that SSE can be reduced by using plates made of materials with low elastic modulus (β titanium alloys, bioresorbable polymers etc.) or by optimization of their 48
49
geometric shape. The latter possibility is analysed in a more detailed way with special 50
51
accent on topology optimization (TO) as a relatively new optimization tool widely used 52
53
by biomedical engineering community. As a practical example, TO using Comsol Multiphysics software is applied to solution of 2D design problem of osteosynthesis 54
55
plate. It is shown that longitudinal stiffness of optimized plate can be reduced up to 84 % relative to initial non-optimized design depending on the value of prescribed 56
57
reduction of weight used as constraint during analysis. Optimized design demonstrates 58
59
increase in maximum von Mises stress, but overall distribution of stresses becomes 57
58
more uniform in comparison with initial design. Prototype of optimized plate can be 58
59
easily manufactured using laser cutting or wire electric discharge machining. 59

Keywords: Osteosynthesis Plates, Stress Shielding Effect, Topology Optimization 60
61



Received:
Accepted:

Copyright: Damascus University- Syria, The authors retain the copyright under a **CC BY- NC-SA**

62 **1. Introduction:**

63 Bone fractures are among the most frequently
64 encountered injuries in the world with more than
65 150 million cases each year. Surgical treatment of
66 bone fractures is based on application of
67 osteosynthesis (bone fixation) plates connected to
68 the bone fragments using screws and ensuring stable
69 relative position of the fragments necessary for their
70 healing. Today bone fixation plates are produced in
71 a wide range of designs depending on anatomical
72 position of fracture, method of fixation and other
73 factors. However, development of new designs of
74 osteosynthesis plates remains actual engineering
75 and medical problem, especially with account for
76 the growing interest in personalized medicine: it is
77 obvious that efficiency of fracture treatment will
78 benefit from application of patient-specific designs
79 of fixation plates considering individual anatomical
80 peculiarities and biomechanical properties of the
81 patient's bones.

82 **2. Literature Review:**

83 One of the main problems related to the use of
84 osteosynthesis plates is so called stress shielding
85 effect (SSE) (Dai, 2004; Gilbert, 1988): application
86 of rigid fixation plates results in protection
87 (shielding) of bone tissue from mechanical stresses
88 typical for healthy bone. SSE can produce adverse
89 effects during fracture healing, particularly
90 osteopenia – reduction of biomineral density
91 (BMD) and strength of bone. Osteopenia related to
92 SSE is a direct consequence of Wolff's law stating
93 that microstructure, biomechanical properties and
94 gross morphology of bones are adapted to the
95 changes in external loads acting on them (Ahn &
96 Grodzinsky, 2009; Boyle & Kim, 2011; Frost,
97 2001). Wolff's law is derived from the observation
98 of German surgeon Julius Wolff, who found out that
99 trabecular bundles in femur bone are directed along
100 the trajectories of principal mechanical stresses.
101 Adaptation of bone to the external loads is more
102 thoroughly described by so called Utah paradigm
103 stating that mechanical stresses produced in bone
104 tissue by these loads are detected by mechanically-
105 sensitive cells (osteocytes) and compared to the
106 prescribed threshold values with lower threshold
107 corresponding to the breakdown (resorption) of

108 bone tissue under insufficient level of loads and
109 upper threshold triggering growth of additional
110 tissue under excessive loading (Frost, 2001). From
111 the microstructural point of view it was found that
112 microcrystals of hydroxyapatite in healthy bone
113 tissue are oriented in preferential direction and in
114 bone subject to SSE this orientation is degraded
115 resulting in reduced BMD (Mie et al., 2020).

116 Selection of fixation plate with optimal stiffness is a
117 compromise problem since, on the one hand, too
118 low stiffness will result in unstable positioning of
119 bone fragments with risk of malunion, but, on the
120 other hand, excessively high stiffness provokes SSE
121 with associated risk of osteopenia and secondary
122 fractures. Ideally plate's stiffness should adapt to
123 the changes of bone biomechanical properties
124 during healing process: in the terminal stages of
125 healing stiffness can be reduced, because fusion of
126 bone fragments precludes their relative
127 displacements. Gradual reduction of plate's stiffness
128 during fracture healing is inherent property of plates
129 made of biodegradable materials like magnesium or
130 bioresorbable polymers (Sheikh et al., 2015;
131 Gaynetdinova et al., 2018). However, rate of
132 material degradation should be matched to the speed
133 of bone healing and, since the latter factor is
134 somewhat unpredictable (patient-specific),
135 application of biodegradable plates does not
136 guarantee optimal outcomes of treatment. So called
137 "dynamizable plates" provide possibility of
138 externally-controlled stepwise reduction (switching)
139 in plate's stiffness upon formation of sufficiently
140 reliable fusion between bone fragments (Dichio et
141 al., 2020). Switching time is selected depending on
142 the speed of bone healing and for this reason
143 dynamizable plates enable patient-specific treatment
144 protocol: however, this advantage is achieved at the
145 expense of structural complexity.

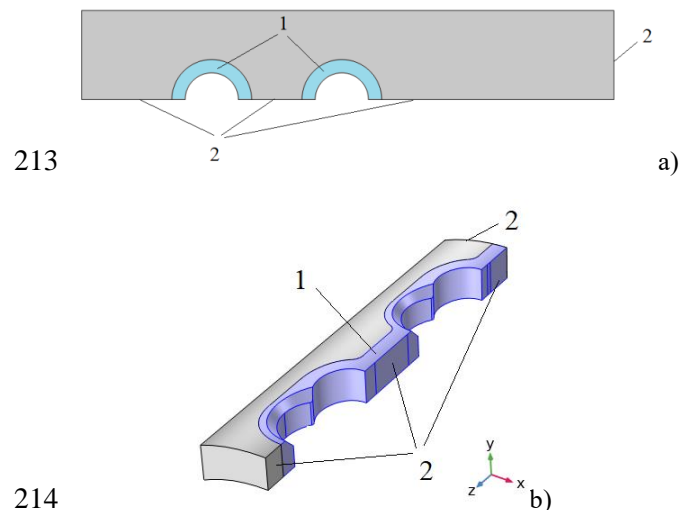
146 Since plate's stiffness depends both on material
147 properties and geometric shape and dimensions of
148 the plate, possibility of variations in geometric
149 shape provides additional flexibility in the design of
150 plates, especially when material choice is limited
151 due to biomedical or technological constraints. In
152 structural design there are two main approaches to
153 the creation of optimally-shaped objects: shape
154 optimization and topology optimization (TO). In

155 contrast to shape optimization TO not only varies
156 shapes of existing object boundaries, but also allows
157 for creation of new internal boundaries (“holes”) or
158 vanishing of existing internal boundaries or, in other
159 words, allows for the changes in object’s topology
160 (Bendsøe & Sigmund, 2003). Optimality of the final
161 topology is qualitatively evaluated in terms of the
162 certain objective function related to the performance
163 efficiency of the object and taking maximum or
164 minimum value for the optimal topology.
165 Frequently used objective functions in mechanical
166 engineering are stiffness (under certain kind of
167 external load, e.g. extensional or flexural load) and
168 total energy of elastic deformation (TEED). These
169 objective functions are equivalent and design with
170 maximum stiffness will have minimum value of
171 TEED. From the practical point of view TO enables
172 design of structures with reduced weight (in
173 comparison to initial non-optimized design) with
174 high performance efficiency, e.g. high stiffness.
175 Successful application of TO is closely related to
176 modern advances in precision numerically-
177 controlled methods of additive manufacturing
178 capable for production of objects with arbitrarily
179 complex shapes.
180 Today TO is widely used in design of medical
181 implants including osteosynthesis plates (Wu et al.,
182 2021). Existing TO methods generally rely on finite
183 element meshing of design domain and include
184 method of evolutionary structural optimization
185 (ESO), method of homogenization and density-
186 based methods. ESO is based in iterative removal of
187 “insufficiently used” finite elements from design
188 domain: for TEED objective function elements are
189 classified as insufficiently used if they have low
190 mechanical stresses (Xie & Steven, 1997). Method
191 of homogenization is used for multiphase composite
192 materials, e.g. laminates and cellular materials. In
193 this method shape of the object remains unchanged
194 and optimization is achieved by spatial variation of
195 effective (volume-averaged or homogenized)
196 properties of composite depending on phase content
197 and design of unit cell (for cellular materials).
198 Density-based methods introduce dimensionless
199 pseudodensity variable θ assigned to each finite
200 element in design domain and taking values from θ

201 = 0 (absence of material) to $\theta = 1$ (solid material).
202 Optimized design is described in terms of associated
203 pseudodensity distribution. More detailed
204 description of optimization method used in the
205 present study will be given in Material and Methods
206 section.

207 3. Material and Methods:

208 TO using density method was implemented for 2D
209 and 3D problems of osteosynthesis plates design
210 using Comsol Multiphysics software. Design
211 domains (initial non-optimized designs) are
212 presented in figure 1.



213
214
215 Figure 1 – Design domains for 2D (a) and 3D (b)
216 problems

217 Geometric symmetry of the plates was accounted by
218 considering incomplete quarter-models with
219 symmetry boundary conditions (roller constraints)
220 applied to the midlines/midplanes 2. Overall
221 dimensions were $180 \times 30 \times 3$ mm for 2D model
222 and $94 \times 13.5 \times 3.5$ mm for 3D model (for complete
223 models). To preserve shape, dimensions and
224 positions of screw openings during optimization
225 they were surrounded with the areas of prescribed
226 material density (APMDs) $\theta = 1$ (denoted as 1 in
227 figure 1). Modelling was implemented for 218
228 titanium alloy (metastable β titanium alloy with
229 composition Ti–15Mo–3Nb–3Al–0.2Si in weight
230 percent). Alloys of this kind are prospective for
231 applications in biomedical implants due to their

232 biocompatibility, high strength and low elastic
233 modulus: the latter property is advantageous for
234 reduction of stiffness and SSE (Pesode & Barve,
235 2023; Niinomi & Nakai, 2011). Screw openings
236 were loaded with 35 N tensile load corresponding to
237 compressive load of the same value applied to the
238 bone. In 3D model zero-gap contact between curved
239 bottom surface of the plate and bone surface was
240 modeled using additional boundary condition $\mathbf{u} \cdot \mathbf{n} =$
241 0, where \mathbf{u} is displacement vector, \mathbf{n} is surface
242 normal. TEED objective function subject to
243 minimization was used. Prescribed reduction of
244 weight (PRW) no less than 50 % relative to initial
245 design was used as optimization constraint. To
246 prove convergence of analysis design domain in 2D
247 model was meshed with free triangular mesh with
248 maximum element size varying from 3/2 mm
249 (coarse mesh) to 3/16 mm (fine mesh) with two
250 intermediate refinement steps (3/4 and 3/8 mm). 3D
251 model was meshed using free tetrahedral mesh with
252 0.25 mm maximum element size.

253 Optimization was performed using SIMP method
254 (Solid Isotropic Material with Penalization for
255 intermediate densities) belonging to the density-
256 based methods (Bendsøe & Sigmund, 1999). In this
257 method pseudodensity takes values from $\theta_{\min} > 0$
258 (preset value in Comsol is 10^{-3}) to $\theta_{\max} = 1$ and
259 elastic modulus is expressed as

$$260 E = E_{\min} + (E_0 - E_{\min}) \cdot \theta^p, \quad (1)$$

261 where $p > 1$ is integer penalization exponent, E_0 is
262 elastic modulus of solid material, E_{\min} is elastic
263 modulus for $\theta = \theta_{\min}$.

264 Penalization of intermediate densities ensures that
265 most of the elements in final topology will have
266 pseudodensity $\theta = \theta_{\min}$ (white elements) or $\theta = 1$
267 (black elements). Ideal solution of TO problem
268 should contain only these two kinds of elements,
269 because elements with intermediate values of
270 pseudodensity (grayscale elements) cannot be
271 realized during manufacturing from homogeneous
272 material, where each voxel of the object have only
273 two possible states: presence or absence of material.
274 Grayscale elements can be realized only for
275 composite materials with

276 structurally/compositionally controlled effective
277 properties.

278 For suppression of numerical instabilities (mesh
279 dependency of solution and checkerboard patterns)
280 Comsol Multiphysics uses density filtering by
281 means of low-pass Helmholtz filter of spatial
282 frequencies (Lazarov & Sigmund, 2011). Filter
283 radius r_f is inversely proportional to the spatial cut-
284 off frequency and should be no less than maximum
285 element size e_{\max} in the mesh: in present study we
286 used condition $r_f = 2e_{\max}$.

287 Additional suppression of grayscale elements is
288 achieved using hyperbolic tangent projection filter
289 which can be considered as regularized Heaviside
290 step function with smoothed transition between the
291 ranges of zero and unit values (Guest et al., 2011).
292 Projection filter is described using parameter β :
293 increase of β results in more steep transition and
294 more efficient suppression of intermediate values of
295 pseudodensity.

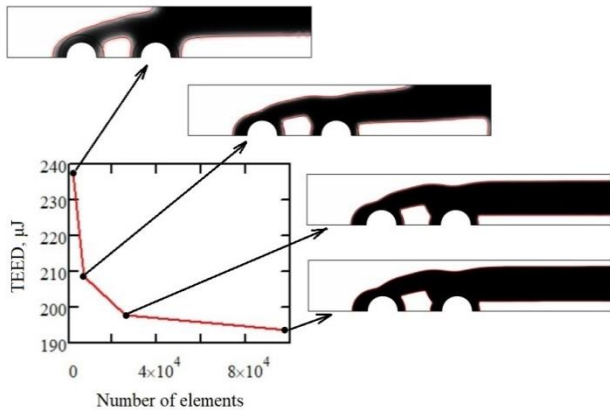
296 In summary Comsol Multiphysics has 4 density
297 variables (listed in the order of their computation):
298 θ_c – initial density (before penalization, filtering and
299 projection), θ_f – filtered density, θ – projected
300 density, θ_p – penalized density. Speed of
301 convergence and quality of solution (number of
302 grayscale elements) are controlled using two
303 parameters: penalization exponent p and projection
304 filter slope β . Increase of these parameters produces
305 solutions of better quality, but slows down
306 computation process. Well-known solution of this
307 problem consists in so called adaptive continuation
308 (Guest et al., 2011): initial low-quality solution is
309 obtained for low values of p and β and then used as
310 non-trivial initial approximation for subsequent step
311 with higher values of p and β producing solution of
312 better quality – this process can be iteratively
313 repeated. In present study we used 4 iterations with
314 the following values of p and β : (1, 2), (2, 4), (3, 6),
315 (4, 8).

316 4. Results and Discussion:

317 Convergence of solution for 2D problem is
318 illustrated by figure 2.

319 During gradual increase in the number of finite
320 elements (corresponding to reduction of their

321 maximum size from 3/2 to 3/16 mm) TEED
 322 approaches stable value and final topology becomes
 323 very close to binary (black and white) design with
 324 minimum number of grayscale elements.



325
 326 Figure 2 – Results of convergence study for 2D model

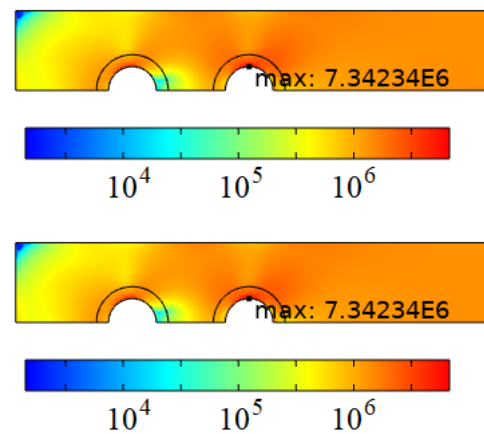
327 Variations in the shape of optimized plates are
 328 negligibly small in the 4th step relative to the 3rd
 329 one and more evident if compare final result with
 330 preceding steps with coarser mesh. Overall shape of
 331 optimized plate is in good agreement with results of
 332 similar studies (Gaynetdinova et al., 2018; Gogarty
 333 & Pasini, 2015).

334 To perform static analysis of generated topology we
 335 extracted isolines of penalized density $\theta_p = 0.2$ as
 336 discrete sets of points and used them for creation of
 337 continuous interpolation curves describing
 338 boundaries of the plate with optimized design.
 339 Optimized plate has shown 36 % reduction in
 340 longitudinal stiffness relative to initial design and,
 341 as a result, will produce less pronounced SSE. On
 342 the other hand, optimized design has maximum
 343 stiffness for the given value of weight. Prototypes of
 344 the plates can be easily manufactured using laser
 345 cutting or wire electrical discharge machining
 346 (EDM). Wire EDM has some advantages over laser
 347 cutting since it produces precise cuts with high
 348 surface quality and generates no heat affected zone.
 349 However, due to technological limitations we used
 350 laser cutting with subsequent plasma electrolytic
 351 etching to improve surface quality. As-cut sample is
 352 shown in figure 3.



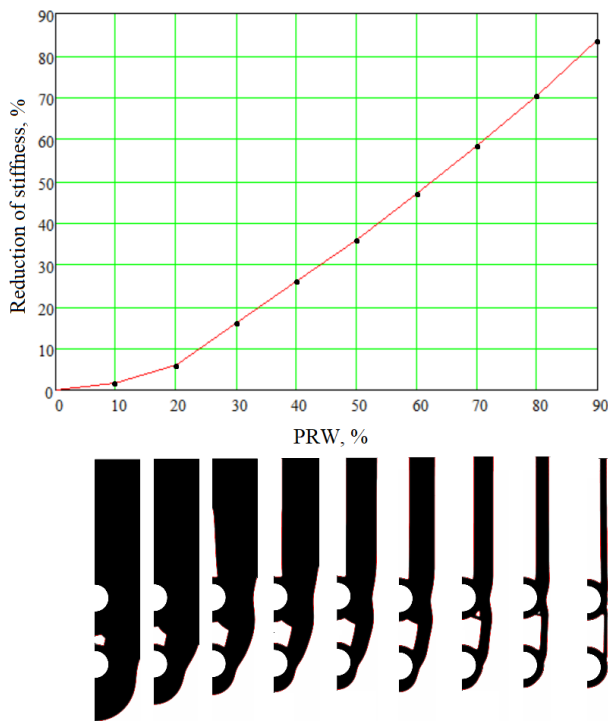
353
 354 Figure 3 – Laser-cut prototype of the plate

355 Optimized plate shows around 20 % increase in
 356 maximum von Mises stress, however it
 357 demonstrates more uniform overall distribution of
 358 stresses (figure 4, for better visual perception
 359 stresses are shown on logarithmic scale).



360
 361
 362 Figure 4 – Distribution of stresses (Pa) in initial (a) and
 363 optimized (b) designs of the plate

364 Effect of PRW constraint on topology and stiffness
 365 of optimized plates is illustrated in figure 5.
 366 As in the case of ESO, optimization firstly removes
 367 least stressed regions of the plate situated at the
 368 corners and near distal (relative to the transverse
 369 midline) openings (blue and cyan regions in figure
 370 4a). By varying PRW value one can produce
 371 designs with stiffness reduced up to 84 % relative to
 372 initial design. It should be noted that real reduction
 373 of weight will be somewhat lower than its expected
 374 value given by PRW, e.g. 47.3 % at PRW = 50 %
 375 and 85 % at PRW = 90 %. The reason is that real
 376 design is produced from simulated grayscale
 377 topology using thresholding (with condition $\theta_p \geq$
 378 0.2) and some low-density “grey” elements are
 379 interpreted during this procedure as solid material.



380

381 Figure 5 – Topology and stiffness of the plates as a
382 function of PRW constraint

383 Optimization results for 3D model will be presented
384 in the future studies. However, in conclusion we
385 would like to highlight some fundamental
386 differences in methodology of 3D TO.

387 The main drawback of 2D model is simplified
388 representation of screw openings. Simple
389 cylindrical openings are rarely used, e.g. locking
390 compression plates are manufactured with
391 complexly-shaped combined openings (figure 1b)
392 providing possibility to use two kinds of screws:
393 compression screws with spherical heads ensuring
394 compression of bone fragments and locking screws
395 with threaded conical heads ensuring angular
396 stability of the plate in the case of its implantation
397 with a gap relative to the bone surface (Cronier et
398 al., 2010) (implantation of this kind preserves
399 normal vascularization of periosteum; thread is
400 removed in finite element model to avoid
401 excessively dense meshing). Complex shape of
402 screw openings dictates the need for more complex
403 (in comparison with 2D model) geometry of APMD
404 (denoted as 1 in figure 1b). In 2D model each screw
405 opening is surrounded with its own APMD and

406 individual APMDs are not connected to each other.
407 In 3D model utilization of separated APMDs
408 resulted in the loss of connectivity in the final
409 topology: design domain was broken down into
410 several subdomains not connected to each other. To
411 avoid this problem APMDs should be “bridged”
412 together in 3D model with formation of single
413 APMD: however, there are different possible
414 topologies of such bridging and their effect on final
415 solution should be additionally studied.

416 Another important difference is related to
417 verification of TO results. For both 2D and 3D
418 models verification is performed by means of static
419 analysis of optimized design. However, we have to
420 use different approaches to transform distribution of
421 pseudodensity produced by TO into the model
422 appropriate for static analysis. As it was described
423 earlier, for 2D model this task is implemented by
424 extracting isolines of penalized material density θ_p .
425 For 3D model this approach was found to be
426 unfeasible, because irregular shape (particularly,
427 lack of smoothness) of extracted isosurfaces
428 resulted in hard-to-fix problems: we tried to extract
429 isosurfaces as point clouds with their subsequent
430 transformation into interpolation surfaces and
431 represent isosurfaces as STL meshes, but both
432 methods were unsuccessful. For this reason we
433 came to the idea of performing static analysis on the
434 same mesh as TO, but with spatially-dependent
435 material properties (elastic modulus and density).
436 To describe this dependence we represented
437 distribution of θ_p obtained from solution of TO
438 problem as 3D interpolation function and assigned
439 material properties depending on the values of this
440 function: similarly to equation (1) low values of θ_p
441 were mapped into the values of elastic modulus and
442 density essentially smaller than corresponding
443 properties of the solid material.

444 5. References:

445 Dai, K. (2004). Rational utilization of the stress
446 shielding effect of implants. In: *Biomechanics and*
447 *Biomaterials in Orthopedics*. Springer-Verlag
448 London. 208-215.

449 Gilbert, J.A. (1988). Stress protection osteopenia
450 due to rigid plating. *Clinical Biomechanics*, 3(3),
451 179-186.

452 Ahn, A.C., & Grodzinsky, A.J. (2009). Relevance of
453 collagen piezoelectricity to "Wolff's law": a critical
454 review. *Medical Engineering & Physics*, 31, 733-
455 741.

456 Boyle, C., & Kim, I.Y. (2011). Three-dimensional
457 micro-level computational study of Wolff's law via
458 trabecular bone remodeling in the human proximal
459 femur using design space topology optimization.
460 *Journal of Biomechanics*, 44, 935-942.

461 Frost, H.M. (2001). From Wolff's law to the Utah
462 paradigm: insights about bone physiology and its
463 clinical applications. *The Anatomical Record*,
464 262(4), 398-419.

465 Mie, K. et al. (2020). Impaired bone quality
466 characterized by apatite orientation under stress
467 shielding following fixation of a fracture of the
468 radius with a 3D printed Ti-6Al-4V custom-made
469 bone plate in dogs. *PLoS One*, 2020, e0237678.

470 Sheikh, Z. et al. (2015). Biodegradable materials for
471 bone repair and tissue engineering applications.
472 *Materials*, 8, 5744-5794.

473 Gaynetdinova, A.A. et al. (2018). Topology
474 optimization of forearm osteosynthesis implants
475 based on biodegradable polymers. In: *XXX*
476 *International Conference of Young Scientists and*
477 *Students "Topical Problems of Mechanical*
478 *Engineering 2018"*, 20-23 November 2018,
479 Moscow, Russian Federation. (In Russian)

480 Dichio, G. et al. (2020). Engineering and
481 manufacturing of a dynamizable fracture fixation
482 device system. *Applied Sciences*, 10, 6844.

483 Bendsoe, M.P., & Sigmund, O. (2003). *Topology*
484 *optimization: theory, methods and applications*.
485 Springer.

486 Wu, N. et al. (2021). The advances of topology
487 optimization techniques in orthopedic implants: a
488 review. *Medical & Biological Engineering &*
489 *Computing*, 59, 1673-1689.

490 Xie, Y.M., & Steven, G.P. (1997). *Evolutionary*
491 *structural optimization*. Springer-Verlag London.

492 Pesode, P., & Barve, S. (2023). A review –
493 metastable β titanium alloy for biomedical
494 applications. *Journal of Engineering and Applied*
495 *Science*, 70, 25.

496 Niinomi, M., & Nakai, M. (2011). Titanium-based
497 biomaterials for preventing stress shielding between
498 implant devices and bone. *International Journal of*
499 *Biomaterials*, 2011, 836587.

500 Bendsoe, M.P., & Sigmund, O. (1999). Material
501 interpolation schemes in topology optimization.
502 *Archive of Applied Mechanics*, 69, 635-654.

503 Lazarov, B.S., & Sigmund, O. (2011). Filters in
504 topology optimization based on Helmholtz-type
505 differential equations. *International Journal for*
506 *Numerical Methods in Engineering*, 86, 765-781.

507 Guest, J.K. et al. (2011). Eliminating beta-
508 continuation from Heaviside projection and density
509 filter algorithms. *Structural and Multidisciplinary*
510 *Optimization*, 44, 443-453.

511 Gogarty, E., & Pasini, D. (2015). Hierarchical
512 topology optimization for bone tissue scaffold:
513 preliminary results on the design of a fracture
514 fixation plate. In: *Engineering and Applied Sciences*
515 *Optimization*. Springer. 311-340.

516 Cronier, P. et al. (2010). The concept of locking
517 plates. *Orthopaedics & Traumatology*, 96S, S17-
518 S36.